Atmos. Chem. Phys. Discuss., 15, 15755–15790, 2015
www.atmos-chem-phys-discuss.net/15/15755/2015/
doi:10.5194/acpd-15-15755-2015

Atmospheric Chemistry and Physics Discussions

Improving aerosol interaction with clouds and precipitation in a regional chemical weather modeling system

C. Zhou, X. Zhang, S. Gong, Y. Wang, and M. Xue

Institute of Atmospheric Composition, Chinese Academy of Meteorological Sciences, China Meteorological Administration (CMA), Beijing 100081, China

Received: 30 April 2015 – Accepted: 19 May 2015 – Published: 12 June 2015

Correspondence to: C. Zhou (zhouch@cma.gov.cn)

Published by Copernicus Publications on behalf of the European Geosciences Union.

Abstract

A comprehensive aerosol–cloud–precipitation interaction (ACI) scheme has been developed under CMA chemical weather modeling system GRAPES/CUACE. Calculated by a sectional aerosol activation scheme based on the information of size and mass from CUACE and the thermal-dynamic and humid states from the weather model GRAPES at each time step, the cloud condensation nuclei (CCN) is fed online interactively into a two-moment cloud scheme (WDM6) and a convective parameterization to drive the cloud physics and precipitation formation processes. The modeling system has been applied to study the ACI for January 2013 when several persistent haze-fog events and eight precipitation events occurred.

The results show that interactive aerosols with the WDM6 in GRAPES/CUACE obviously increase the total cloud water, liquid water content and cloud droplet number concentrations while decrease the mean diameter of cloud droplets with varying magnitudes of the changes in each case and region. These interactive micro-physical properties of clouds improve the calculation of their collection growth rates in some regions and hence the precipitation rate and distributions in the model, showing 24 to 48 % enhancements of TS scoring for 6 h precipitation in almost all regions. The interactive aerosols with the WDM6 also reduce the regional mean bias of temperature by 3 °C during certain precipitation events, but the monthly means bias is only reduced by about 0.3 °C.

1 Introduction

Hygroscopic aerosols can act as cloud condensation nuclei (CCN) or ice nuclei (IN) to participate in cloud formations, alter the microphysics and life time of clouds and then impact the precipitations (Twomey, 1977; Albrecht, 1989; Seinfeld and Pandis, 1997; Ramanathan et al., 2001), which is so-called aerosol cloud interactions (ACI). Most of the previous researches on ACI focus on single clouds or climate impacts with

ACPD
15, 15755–15790, 2015

very limited numbers on the meso-scale weather, partially due to the difficulties to establish real and reasonable connections from emissions to aerosol, CCN, clouds and then precipitations. Aerosols, impacted by emission, processes of microphysics and atmospheric thermo-dynamics, are in different size ranges and consisted of several components which are often temporally and spatially varied (Jacobson et al., 1994; Zhang et al., 1999; Gong et al., 2003; X. Y. Zhang, et al., 2012). Some components, such as organic carbon (OC), are in very complex structures and many of their precursors still cannot be detected (Stockwell et al., 1997; Jacobson et al., 2000; Fuzzi et al., 2006). Meanwhile clouds are also the results of complex interactions among atmospheric thermo-dynamics of different processes. The scale of aerosol–cloud interactions spans from nanometer to thousand kilometers including both complex microphysics and scales of clouds and aerosols and macrophysics of air mass and atmospheric circulations. All of these make it very difficult to establish a direct connection from emission to precipitation to quantify the effects of aerosol on clouds and precipitations in both climate and weather models (Lohmann and Feichter, 2005; Khain, 2009; Stevens and Feingold, 2009; Tao et al., 2012).

A numerical weather model with aerosol feedbacks is an important and effective way to explore the interactions between aerosols, clouds and precipitation (Yin et al., 2002; Khain, 2009; Levin and Cotton, 2009; Tao et al., 2012). Currently, two distinct approaches, the bin method and the bulk method, are often used to explore cloud microphysics in atmospheric models. For bin models, each type of cloud hydrometers is sectionally resolved to represent their mass or size distributions which might be changed in the course of the model integration (Khain and Sednew, 1996; Khain et al., 2004). The bin methods can explicitly resolve cloud microphysics and provide very rigorous solution than bulk approach, but they are limited to single clouds because of huge computation. The bulk models have been improved from single-moment approach to two-moment approach. The two-moment models can predict not only mass but number concentrations which allow more flexibility of the size distribution and enable the mean

ACPD
15, 15755–15790, 2015

diameter to evolve in contrast with the single-moment method (Seifert and Beheng, 2001; Morrison et al., 2005; Lim and Hong, 2010).

However, no matter which cloud approach is used, the relationship between aerosol and cloud droplet needs to be established. One of the existing relationships is the Twomey approach which links the cloud droplet number concentration to aerosol number concentration (N_0) by two simplified parameters and has been widely used in climate and weather models (Twomey, 1959; Boucher, 1995; Gultepe and Isaac, 1996; Khairoutdinov and Kogan, 2000; Ramanathan et al., 2001). In this approach, N_0 and a parameter κ represent the capability of aerosol activation and vary from regions to regions with certain value. N_0 has been roughly classified into four zones: rural, urban, ocean and remote continents with no connections to the emissions and production of the actual aerosol distribution in most cases and with no physical processes of aerosol activations, i.e. CCN. Even though in some models CCN can be prognostic as a result of advection, activation and scavenging (Yin et al., 2002; Khain et al., 2004; Fan et al., 2012), aerosol size distribution and the total aerosol number have to be prescribed. This may introduce additional bias into aerosol and cloud interaction, especially for regions with high aerosol concentration and diverse compositions like China.

East China is one of the most polluted areas in the world (X. Y. Zhang, et al., 2012). High accumulated aerosols and stagnant weather systems frequently form the regional haze-fog evens there (R. H. Zhang, et al., 2013; X. Y. Zhang, et al., 2013; Che et al., 2014; Horton et al., 2014). Heavy aerosol pollution has been related to the decrease precipitation and the cooling radiative effect elsewhere (Cheng et al., 2005; Zhao et al., 2006; Ma et al., 2010; Wang et al., 2015). Several studies by two-moment scheme with the highly parameterized scheme Twomey formula or by bin model for one cloud show that microphysics of different regimes of clouds and precipitation can be more realistically simulated by adding aerosol impacts in China (Zhang et al., 2007; Yang et al., 2011; Fan et al., 2012; Guo et al., 2014). Since high aerosol concentrations alter the radiation, cloud microphysics and then the precipitation, its impacts on weather systems cannot be ignored in regional weather models.

ACPD
15, 15755–15790, 2015

In order to take into account of the effects of aerosol on cloud and precipitation, a comprehensive scheme containing the emission, aerosols, clouds and their interaction mechanisms has been developed in GRAPES/CUACE. It is built on the base of the China Meteorological Administration (CMA) Unified Atmospheric Chemistry Environment/Aerosol (CUACE/Aero) (Zhou et al., 2012), and the CMA weather forecasting model called Global/Regional Assimilation and PrEdiction System–GRAPES (Chen et al., 2008). By integrating a time dependent CCN formulation from an aerosol activation scheme with active aerosol size and composition information directly from CUACE, it enables the quantitative assessment of the impacts of aerosol pollution on clouds and precipitation.

By developing and using the ACI scheme in GRAPES/CUACE here, the aerosol impacts on clouds and precipitations in east China have been investigated for 1–31 January 2013 when a series of long lasting haze-fog episodes hit this region and eight precipitation events also occurred. This paper has divided into five sections, beginning with Sect. 2 for the description of the modeling system: GRAPES/CUACE. Case description and numerical experiments designs are in Sect. 3. Results and discussions will be shown in Sect. 4, followed by Sect. 5: Conclusions.

2 ACI scheme established in GRAPES/CUACE

2.1 GRAPES/CUACE system

The CMA new generation of weather forecasting model GRAPES is a fully compressible non-hydrostatical weather model systems by using a semi-implicit and semi-Lagrangian discretization scheme (Chen et al., 2008; Xu et al., 2008; Zhang and Shen, 2008). It uses a Arakawa C staggered grid and the central finite-difference approach of second-order accuracy in horizontal coordination, a nonhydrostatic approximation method together with the staggered approach of Charney–Phillips to improve the accuracy of vertical pressure gradients and a semi-implicit and semi-Lagrangian scheme for

ACPD
15, 15755–15790, 2015

temporal and advection discretion. A height-based terrain following coordinate, which behaves as a natural height coordinate, is used to compromise the Lagrangian trajectory errors in spherical coordinates at high latitudes. The physical packages include cumulus convective, single moment cloud microphysics, radiative, land surface and boundary layer processes.

CUACE is a unified atmospheric chemistry environment with four major functional sub-systems: emissions, gas phase chemistry, aerosol microphysics and data assimilation. It is designed to facilitate the establishment of a chemical weather forecasting system using near real time data in China (Zhou, et al., 2008, 2012). Seven aerosol components, i.e. sea salts, sand/dust, elemental carbon, organic carbon, sulfates, nitrates and ammonium salts are sectioned in 12 bins with detailed microphysics of hygroscopic growth, nucleation, coagulation, condensation, dry depositions and wet scavenging in the aerosol module. The gas chemistry module is based on the second generation of Regional Acid Deposition Model (RADM II) mechanism with 63 gaseous species through 21 photo-chemical reactions and 121 gas phase reactions applicable under a wide variety of environmental conditions especially for smog (Stockwell et al., 1990) and prepares the sulfate and production rate of secondary organic aerosol for the aerosol module.

CUACE is fully online coupled to the regional version of GRAPES to establish the comprehensive modeling system – GRAPES/CUACE and has been used for radiative feedback researches (Wang et al., 2010, 2015).

2.2 Aerosol activation scheme HG

The sectional aerosol activated scheme developed by Hayder Abdul-Razzak and Ghan (HG scheme) provides a convenient platform to connect sectional aerosols into cloud physics (Ghan et al., 1993, 1995; Abdul-Razzak et al., 1998; Hayder and Ghan, 2000; Abdul-Razzak and Ghan, 2002). This scheme is derived from the basic theory of Köhler curve to calculate how a particle can be activated under a certain supersaturation in an air parcel. The newly activated CCN would be parameterized in terms of environmental

ACPD
15, 15755–15790, 2015

supersaturation and the upper and low limit of the critical supersaturation for each aerosol bin. This method is very useful for precise determination of concentration of droplets nucleated at the cloud base. However, droplet nucleation or aerosol activation can also take place above the cloud base as well, which is induced by increasing supersaturation above cloud base and lateral entrainment of the surrounding air with dry aerosols (Khain et al., 2000). Therefore, it is not enough to calculate the CCN at the cloud base only in an air parcel, especially for stratus clouds where turbulence is more important than the vertical movement (Bodenschatz et al., 2010). For these reasons, the HG scheme has been online coupled with both the stratus scheme and the convective scheme in GRAPES. Consequently, Aerosols from CUACE can be activated into CCN as the humid condition is satisfied, not just in the cloud base.

2.3 Aerosol activation in Warm Double-Moment 6 scheme

The WRF Double-Moment 6-class scheme (WDM6) is introduced into GRAPES since it can predict not only the mass but also the number of droplets and drops (Lim and Hong, 2010). It is developed from the WRF Single-Moment 6-class scheme (WSM6) and needs the CCN input for cloud droplets which provides a direct way for aerosol feedbacks into clouds and precipitation. The original activation scheme is expressed as (K2000) (Twomey, 1959; Khairoutdinov and Kogan, 2000):

$$n_a = (n + N_c)\left(\frac{S_w}{S_{\max}}\right)^{\kappa} \tag{1}$$

The change rate of cloud droplet number concentration due to CCN activation is given by:

$$\frac{\partial N_c}{\partial t} = \frac{\max\left\{0, (n + N_c)\min\left[1, \left(\frac{S_w}{S_{\max}}\right)^{\kappa}\right] - N_c\right\}}{\Delta t} \tag{2}$$

ACPD
15, 15755–15790, 2015

Three unknown parameters in this activation scheme: aerosol number concentration n, activation parameter κ and max supersaturation S_{max} are usually preset just like the way Twomey formula does with the inherited shortcomings due to the insufficient information of real aerosols. To overcome these shortcomings, the aerosol size and composition information from CUACE and the humid and thermal information from GRAPES are used in HG scheme to calculate the CCN production rate at each time step, which is then fed into WDM6 to replace the CCN production rate by the scheme of K2000.

An aerosol particle can be quickly activated into CCN, usually in less than a second, as the atmosphere reaches the critical supersaturation of the aerosols (Kogan, 1991). In models with relatively coarse resolution like GRAPES, supersaturation cannot be easily satisfied because of the insufficient information of inhomogeneous turbulence and vertical movements even when the grid-mean relative humidity is over about 85–90 %. While local supersatureation around a particle can be satisfied through which clouds can be formed. As the local supersatureation is not only decided by the mean fields, a parameterized scheme has been developed to add the effect of local turbulence and vertical movements to the supersaturation in HG scheme for WDM6 in GRAPES. The turbulence effect is assumed to be proportional to the mean relative humidity and inversely proportional to both the horizontal wind speed and the vertical height.

2.4 Aerosol activation in KF scheme

Stratiform and convective precipitations are the two precipitation regimes that cannot be mutually excluded. The former refers to those precipitations with low vertical motions and the later with stronger ones (Houze, 1997). These two regimes can be fully explicit in meso-scale model only under the condition that the model resolution is below several hundred meters (Molinari and Dudek, 1992), which is very difficult to realize for the online coupled modeling systems such as GRAPES/CUACE. A hybrid approach is often used in most meso-scale models which can explicitly condense water for the stratus

ACPD
15, 15755–15790, 2015

precipitation in grid scale, to parameterize convective scale precipitation in sub-grid. In order to fully account the ACI in the model, HG scheme has also been coupled to the Kain–Fritch convective parameterization scheme (KF) in GRAPES/CUACE (Fritsch and Chappell, 1980; Kain and Fritsch, 1990; Kain, 2003). The sectional aerosols have been introduced and moved upward or downward as the air mass does in KF. They would be activated as soon as the supersaturation satisfies the critical supersaturation by HG scheme.

Since there is no size information for cloud and rain water in the bulk convective scheme, a generalized gamma distribution has been introduced to describe the cloud-droplet and raindrop spectra (Clark, 1974; Walko et al., 1995; Cohard and Pinty, 2000).

$$N_X(D_X) = N_X \frac{\alpha_X}{\Gamma(\nu_X)} \lambda_X^{\alpha_X \nu_X} D_X^{\alpha_X \nu_X - 1} \exp\left[-(\lambda_X D_X)^{\alpha_X}\right] \quad (3)$$

$\lambda_X = \left[\frac{\pi}{6}\rho_w \frac{\Gamma(\nu_X+3/\alpha_X)}{\Gamma(\nu_X)} \frac{N_X}{\rho_a r_X}\right]$, $N_X = N_0 + N_{\mathrm{ccn}}$, N_{ccn} is the newly activated aerosol number concentration, N_0 is the cloud number concentration which is set to be 30 cm^{-3} in terms of observations at autumn in east China (Zhang et al., 2011; Y. Zhang, et al., 2012). Normally α_X can be specified priori as 1 for number concentration size distribution and 3 for mass concentration size distribution. One parameter ν_X left has to be tuned through measurements. A parameterization for ν_X has been proposed through the total droplet number concentration and liquid water content (Geoffroy et al., 2010):

For size spectra of number concentration:

$$\alpha_X = 1, \quad \nu_X = 14.5 q_c + 6.7 \quad (4)$$

For size spectra of mass concentration:

$$\alpha_X = 3, \quad \nu_X = 1.58 q_c + 0.72 \quad (5)$$

In Eqs. (4) and (5), q_c is the liquid water content in the unit of $\mathrm{g\,m}^{-3}$. With Eqs. (4) and (5), droplet size distribution in Eq. (3) can be bulky represented by the total liquid

ACPD
15, 15755–15790, 2015

water content and total cloud droplet number concentration which can then include the newly activated aerosols from HG.

The condense of KF scheme is allowed to be removed as precipitation based on an empirical relationship (Ogura and Cho, 1973).

$$\delta r_c = r_{co}(1 - e^{-c_1 \delta z / w}) \quad (6)$$

The precipitable water δr_c is inversely proportional to the vertical velocity w, which means that a small vertical velocity would produce more δr_c. As smaller vertical velocity means weaker convection and less r_{co}, less precipitable water δr_c would be produced. Therefore, r_{co} and w are offset each other, which may cause false large convective precipitation. In order to overcome this problem, the size spectrum information of cloud drops and droplet are introduced into the convective clouds, which resolves the total cloud water content and number concentrations including the newly formed CCN. The new precipitable rain water, named as r_p, can be calculated by integrating Eq. (3) to replace r_{co} in Eq. (6). The threshold for cutoff radius between the droplets and rain drops in the integration is 50 µm for deep convective precipitation (Berry and Reinhardt, 1974; Seifert and Beheng, 2001), and 25 µm for shallow convective precipitation (Khairoutdinov and Kogan, 2000). Terminal velocity w_T for the rain drops has also been introduced. Finally, Eq. (6) is reformed as:

$$\delta r_c = r_p(1 - e^{-w_T / w}) \quad (7)$$

Now, the comprehensive interactions of aerosol–cloud–precipitation have been established in GRAPES/CUACE with activated aerosols from CUACE linked into both the stratus and convective clouds to participate in the cloud and precipitation processes.

ACPD
15, 15755–15790, 2015

3 Case description and numerical experiment designs

3.1 Case description

A series of long-lasting heavy haze-fog events hit east part of China in January 2013. Climatology analysis shows that the mean number of the hazy days is much higher than the mean value from 1981 to 2010, especially in the three major pollution zones of North Plain, Delta of Yangtze River and Zhu River (R. H. Zhang, et al., 2013). Meanwhile, the values of the stagnant polluted parameter PLAM, a threshold value to distinguish clear and polluted weather, are over 80 in most part of east China, which indicates strong static weather conditions for pollutant accumulation (Wang et al., 2012; X. Y. Zhang, et al., 2013). Surface daily mean $PM_{2.5}$ concentrations are in the range of 100–150 $\mu g\,m^{-3}$ and AOD is above 1.0 in many surface stations (Che et al., 2014; Wang et al., 2014).

Eight precipitation events also occur in January 2013 with six of them sweeping over regions south of Yangzi River as every low pressure system moving out of Sichuan Basin (Table 1). Other two cases are related to the cold fronts and affect the whole east of China. This forms a very good period to study ACI under high pollution conditions.

3.2 Numerical experiment designs

Three sets of experiential runs are designed: T1 with the single-moment microphysics scheme of WSM6 and original KF without aerosol activation; T2 with WDM6 scheme and the activation scheme K2000 and T3 with HG activation scheme online connected with WDM6, KF and CUACE. Five target regions are selected for the evaluation in terms of typical heavy pollution regions over China (Fig. 1). R1 and R2 are covering the whole China and east China respectively. Within R2, R3, R4 and R5 are representative of three typical polluted zones: north east China, North China Plain and south China.

The meteorological initial and boundary conditions are interpolated from the forecasting outputs of the CMA medium Meteorological model T639 in 6 h interval. The

ACPD
15, 15755–15790, 2015

surface daily and hourly $PM_{2.5}$ concentrations from CMA Atmosphere Watch Network (CAWNET) are used to evaluate the performance of aerosols (Zhang et al., 2008, 2011). Precipitation data from the rain gauges in meteorological stations over China are used for the precipitation TS scoring (Wang et al., 2008). Temperature, geopotential height, humidity and cloud water mixing ratio of NCEP reanalysis at standard pressure levels from 1000 to 10 hPa are used as real the atmosphere to evaluate the outputs of GRAPES/CUACE (Kalnay et al., 1996).

4 Results and discussions

In order to quantify the impacts of aerosols on precipitations, the cloud properties such as the total cloud water content, clouds liquid water content and mean droplet diameters are analyzed to elucidate the aerosol's effect on clouds. As hourly changes of the variables above are very chaotic, regional means are discussed in order to avoid the interruption of small scale advection and diffusion. The TS scores of 6 h precipitation are also quantitatively analyzed to evaluate the aerosol's effect on precipitation. The changes in temperature and height are also discussed to explore the aerosol effects on the thermal and dynamics. Hourly surface aerosol concentrations are compared to the measurements to see the ACI feedbacks on aerosol distribution.

4.1 Aerosol effects on the clouds

Regional-monthly-mean vertical profiles of the total cloud water (the total mass of cloud water, rain water, ice water, snow and grauple) and temperature for T1, T2 and T3 together with the NCEP reanalysis in R1, R2, R3, R4 and R5 are shown in Fig. 2a1–a5 and b1–b5. Compared to T1, T2 and NCEP reanalysis in the layers below 600 hPa, the total cloud water all increases obviously in the five regions for T3 with a clear peak at about 850 hPa. These results indicate that with more realistic aerosols interacting

ACPD
15, 15755–15790, 2015

with clouds (T3), more water vapor condenses into cloud water due to the activation of aerosol particles.

The amount of the increasing cloud water for T3 has very unique regional characteristics. The increase in R1, i.e. national wide with plenty of remote areas such as Tibetan and northwest China, is much less than in R2 which represents the most developed regions in China with a lot of emissions. Of the three typical polluted regions within R2, R3 covers most part of northeast China with below-freezing temperature, which is not favorable for warm cloud formation and therefore no obvious increases is found compared between T2 and T3. While the temperature in R4, the most polluted area in China, is near or just above freezing, the condition is favorable for the long lasting haze formation but not a good condition for cloud and precipitation formation with the relatively less cloud water. In R5 where abundant cloud water exists and temperature under 700 hPa is above freezing, this region has the most enhancement for aerosol activation and warm clouds development.

The amount of total cloud water by T1 and T2 is compatible to each other because there is no aerosol feeding into the single moment scheme T1 and the aerosol activation is based on the prescribed aerosol numbers without spatial variation in T2. Profiles of cloud water from NCEP are close to that of T1 and T2 in all of the five regions. Even though the basic variables such as wind, temperature, relative humidity, height and pressure are most analyzed from measurements, the cloud water from NCEP reanalysis is not from direct observations but from cloud physics diagnosis. Cloud water data from NCEP reanalysis should be carefully used in the regions affected by high aerosol concentrations.

For all regions, the increases by T3 in total cloud water contents are driven by liquid water contents (Fig. 3a1–f1). The solid cloud water for T1, T2 and T3 is in the same order of $1.0 \times 10^{-3}\,\mathrm{g\,kg^{-1}}$ in all the three regions and follow almost the same vertical distribution shapes with tiny difference of height and thickness in each region, showing relatively small effects from aerosols (Fig. 3a2–f2).

ACPD
15, 15755–15790, 2015

The aerosols activation in T3 can also increase the cloud number concentrations which affect the mean diameters of droplet (MDD). The profiles of MDD in R4 and R5 are shown in Fig. 4. MDDs for T3 are all below 10 µm, about one order less than those of T2, and change little with height in the lower troposphere under 700 hPa (Fig. 4a), showing a clearly decrease after aerosols activated into clouds in North China Plain (R4) and south China (R5). Conventionally, smaller droplets (usually less than 20 µm) need more time to grow up into rain drops than the larger ones, which should result in more rains produced in T2 than in T3 after a decrease in MDDs. However, due to the self-collection growth process, which depends on both the MDDs and number concentrations of cloud droplets, the simulations in T2 do not see more rain produced (as discussed in Sect. 4.2).

In order to investigate the combined impacts of both MDDs and number concentrations on rain production, the self-collection kernels for the two-moments WDM6 from Long's work (Long, 1974) is used. As showed in Fig. 4e, self-collection rates (SCRs) of R5 for T3 are the largest among all the three tests in the three regions of R3, R4 and R5. They are over 100 $m^{-3} s^{-1}$ under 700 hPa, about one order of magnitude higher than by T2. This indicates that in R5 even though the activated aerosols from CUACE decrease the mean droplet diameters which may in some way decrease the self-collection process, the high concentration of cloud droplets from aerosols activation, four orders of magnitudes higher than that of T2, enhances the chance of collision and compromises the decreasing collision trend by the decreasing diameter. Therefore, the SCRs can explain the phenomenon that the precipitation simulation ability increases obviously for T3 in R5 (in Sect. 4.2). While in North China Plain (R4), SCRs for T3 and T2 are almost the same, varied around the value of 2 $m^{-3} s^{-1}$, meaning that a lot of aerosols activate as a small cloud drops, grow very slowly into larger ones and stay relatively longer in the atmosphere, forming the long lasting haze there (Fig. 4d). In northeast China (R3), SCRs for T3 and T2 are so small that the SCRs could be ignored, which is also consistent with the cold cloud formation (Fig. 4c).

ACPD
15, 15755–15790, 2015

In summary, the aerosol effects on cloud formation are very different in the three typical polluted regions: R3, R4 and R5. As shown above, R3 is controlled by cold cloud formation processes, little effect can be seen in this region. In R4, the relatively humid layer from the surface to 600 hPa indicates a favorable condition for the long lasting haze formation as proved by both the mean diameter of droplets and collection rates. In R5, liquid water for T3 is also one order higher than that in R4 and three orders of magnitude higher than that in R3. Together with the highest collection rate, R5 processes a good condition for precipitation formation, which is consistent with the improvement of the precipitation simulation ability as discussed below.

4.2 Aerosol effects on precipitation

4.2.1 Regional TS scoring evaluation

The TS scoring is a common and useful way to quantitatively evaluate the model performance of regional precipitation (Casati and Ebert, 2009; Mitternaier et al., 2013). The 6 h accumulated gauge values from 1400 routine weather stations in CMA are used for the evaluation. The threshold value for the contingency table is 0.1 cm which is in harmony to the 24 h's TS scoring threshold usually used in most operational weather forecasting centers. TS scoring for 6 h precipitation is more strict than 24 h's due to the short time scale. The model precipitation results from the three tests T1, T2 and T3 are interpolated into the meteorological stations and compared with the observations through the 2×2 contingency table to calculate the TS scores for the five targeting regions: R1, R2, R3, R4 and R5.

The time series of 6 h precipitation TS show that for T3 are consistently higher than those for T2 and T1 for all five regions (Fig. 5a–d) with a monthly-mean improvement of about 33, 45, 32, 24 and 50 % respectively (Fig. 5f–l). The improvement for south China (R5) is the highest which is in consistent with the results of active aerosol effects on clouds there. Even in China North Plain (R4) where only two precipitation events occur and last for only 4 days, the mean TS score of T3 is still higher than that of T1 and T2

ACPD
15, 15755–15790, 2015

(Fig. 5c and i). The monthly mean TS scores for T2 are not higher but slightly lower than that for T1 in R2, R4 and R5, indicating that without the real aerosol information from CUACE, the two-moment scheme cannot improve the model precipitation simulation. There is an exception in R3 where TS of T2 is almost the same with that of T3. This is because that the precipitation is mainly formed by icy clouds in north China (R3) in January and little aerosols can be activated into cloud droplets to participate in the cloud processes, resulting a small TS scoring difference between T2 and T3. It can also indicate that the WDM6 does improve the microphysics for cold cloud formation as the TS scores by T2 and T3 are both higher than that by T1 in R3.

To evaluate the overall performance, false alarm or missing events need to be considered. The monthly biases of precipitation simulation, namely (hits + false alarm)/(hits + misses), which infers the over- (larger than 1) or under- (less than 1) estimates of the rain frequency, are 0.73, 0.75 and 1.13 for T1, T2 and T3 in R1 respectively (Table 2). This means that the underestimation by T1 and T2 has been corrected by adding real aerosol activation in T3. This is also true for cases in R2, R4 and R5. Figure 6 is a very typical precipitation distribution pattern for T1, T2 and T3 and shows that the precipitations by T3 are very close to the surface observation in terms of timing and coverage from 08:00 to 14:00 LST in 3 January by eye-ball comparison. The TS scorings are 0.71 and 0.62 and the biases are 1.35 and 1.19 for T3, showing a relatively stable and good simulation. As for T1 and T2, TS scorings sharply decrease six hours after 08:00 LST. The value of biases indicates that the TS decreasing comes from severe underestimation as they are much lower than 1. In northeast China (R3), biases for T2 and T3 are close to 1 and close to each other. This is also consistent with the results of cloud water and the TS scorings in this region that WDM6 performs well for cold clouds and precipitation than single moment scheme WSM6.

4.2.2 TS scoring for case evaluation

Two national precipitation events (case 7 and 8) hit most part of east China in R2 including R3, R4 and R5 and six ones (case 1 to 6) hit south China in R5 in January 2013

ACPD
15, 15755–15790, 2015

(Table 1). The mean TS score for all the cases is 0.446, 0.246 and 0.287 for T3, T2 and T1 respectively. The mean improvement is about 68.0 % and the most extraordinary improvement is 192.6 % for case 6. TS scores for T2 are generally lower than those for T1 by −14.5 %. These results are also consistent with the conclusions of regional precipitation scores evaluation.

Both the time series TS and the case TS show that the WDM6 scheme alone cannot improve but decrease the ability of precipitation simulation without the real aerosol activation information in the cloud microphysics even though it is more physically based than the one-moment scheme. Additional errors may have been introduced into the model with the prescribed aerosol number concentrations. Only the WDM6 with the real aerosol size and number concentration information activated in the real atmosphere, as in T3, can significantly improve the model precipitation simulation ability.

4.3 Aerosol effects on temperature

Results of regional-mean temperature profiles in the five targeting areas above 700 hPa are almost the same with the NCEP reanalysis (Fig. 2b1–b5). The differences between simulation and NCEP reanalysis are mostly under 700 hPa in all of the five regions and decrease with height. Temperature is 10 and 5 °C higher for all the three tests (T1–T3) than that of NCEP near the surface in R3 and R4, indicating some problems for GRAPES in North China Plain. In south China (R5) the regional-mean temperature profiles are also almost the same as the NCEP reanalysis, showing a good performance of GRAPES over there. Regional mean Difference of temperature for different tests in each region is not very obvious with the highest value of about 0.2 °C near the surface located in south China between T3 and T1. Above the surface or in other regions, the mean temperature difference is not significant (< 0.05 °C). This means that the regional mean temperature changed by the aerosol is not obvious. This is also the case for the geopotential heights.

The time series of differences in the regional mean temperature biases between T3 and T1 and T2 and T1 in the three typical polluted areas (R3, R4 and R5) in east

ACPD
15, 15755–15790, 2015

China at the three layers are shown in Fig. 7. T3 can clearly decrease the temperature biases below 700 hPa at most time in all the three regions. The difference magnitude decreases from 1000 to 700 hPa, showing the clear impact of aerosol below 700 hPa in these layers. The largest decrease is about 3 °C near the surface and about 1 °C even at 700 hPa in R5 during the precipitation event from 19–22 January. The difference is less than 0.5 °C in R3 and R4 at most time. It also shows that T2 increases the biases with the largest increase in R5. Even in some time T2 might decrease the biases but with a less magnitude compared that of T3.

The above analysis also shows that WDM6 with the activation scheme K2000 can introduce errors to the atmospheric temperature fields because of the missing details of aerosol size and component information. The errors would increase with the intensity and frequency of the precipitations. Same as the conclusion from the TS scoring analysis, only the two moment scheme with the real time aerosol activation can reduce the temperature bias and increase the model ability of precipitation simulation.

4.4 Feedbacks on surface aerosol simulation

To realistically simulate the aerosol impacts on clouds, a good performance of $PM_{2.5}$ simulation, including aerosol sizes and vertical distributions, is critical. Due to limited available observations during the simulation period, only daily average of $PM_{2.5}$ concentrations from GRAPES/CUACE have been interpolated and compared with the observations in thirty two stations from CAWNET which have been sorted into the five targeting regions from R1 to R5. Scatter plot for $PM_{2.5}$ simulation for R1, the nationwide region, in Fig. 8a shows that the daily average particle mass concentrations are in a factor of 2 between the observations and model outputs. This is compatible to the simulation ability of particle matters in most models.

Total correlation coefficients for T1, T2 and T3 in R1 to R5 have been plotted in Fig. 8b. Correlation coefficients for R1, R2 and R5 are all over 0.54 for all the three tests. Correlation coefficients for R4 are about 0.48 for the three tests. This shows a relative stable and reasonably performance for $PM_{2.5}$ over these four regions. Corre-

ACPD
15, 15755–15790, 2015

lations coefficients for R3 are only about 0.2 for the three tests showing a relative poor simulation there. These results are compatible with the result by Zhou (2012) for the same region (Zhou et al., 2012). Figure 8b also indicates that the differences of correlation coefficients of the three tests in each region are very small. ACI can increase the correlation coefficient by about 2 % in terms of monthly mean.

5 Conclusions

A comprehensive aerosol–cloud–precipitation interaction model has been developed under the CMA chemical weather modeling system GRAPES/CUACE. Simulations with this comprehensive system show that interacting activated aerosols from CUACE with WDM6 in GRAPES/CUACE clearly increase the total cloud water, liquid cloud water, number concentration of droplets; decrease the mean diameter of the droplets. It is found that the ultimate efficiency of aerosol to clouds and precipitation is controlled by multiple parameters, largely by self-collection growth rates in high aerosol-loading regions.

Studies show that interacting aerosols can obviously increase the model precipitation performance with a TS scoring improvement from 24 to 48 % and correct the obvious underestimation by the control test. It is found the physically based, two-moment cloud physics WDM6 in GRPAES/CUACE can produce rational precipitation results with only realistic interactive aerosol inputs in warm and mixed clouds especially in highly polluted regions. WDM6 can also improve the performance of precipitation in cold clouds compared to the control test with the one-moment scheme WSM6.

It is further found out that the aerosol–cloud–precipitation interactions in GRAPES/CUACE also reduce temperature bias as well, especially under 700 hPa, which is in harmony with the fact that most aerosols locate below this layer. Aerosol–cloud interaction can decrease the temperature bias by 3 °C at some times during the precipitation event. The monthly mean impact by aerosol–cloud interaction is only about 0.3 °C. Aerosol–cloud interaction's feedback to the surface aerosol concentration

ACPD
15, 15755–15790, 2015

is not significant and can increase the correlation coefficient by about 2 % in terms of monthly mean.

In this paper, an ACI scheme has been explored mainly in winter time when convection is not strong and large part of precipitation is from stratified clouds that can be resolved by WDM6. As the comprehensive and complex relations from emission to cloud and precipitation in this paper provides a platform to study the aerosol impacts on meso-scale weather system in a much wider spatial–temporal scale in the future, the ACI at different time with different weather pattern should be investigated in the future.

Acknowledgements. The authors wish to thank for the financial support from the National Basic Program (973) of China (2011CB403404), the National Natural Foundation for Young Scientists of China (1340400501), the science and technology support program (2014BAC16B03) and CMA Innovation Team for Haze-fog Monitoring and Forecasting.

References

Abdul-Razzak, H. and Ghan, S. J.: A parameterization of aerosol activation. 3. Sectional representation, J. Geophys. Res., 107, 148–227, 2002.

Abdul-Razzak, H., Ghan, S. J., and Rivera-Carpio, C.: A parameterization of aerosol activation. 1. Single aerosol type, J. Geophys. Res., 103, 6123–6131, 1998.

Albrecht, B. A.: Aerosols, cloud microphysics, and fractional cloudiness, Science, 245, 1227–1230, 1989.

Berry, E. X. and Reinhardt, R. L.: An analysis of cloud drop growth by collection: Part 2. Single initial distribution, J. Atmos. Sci., 31, 1825–1831, 1974.

Bodenschatz, E., Malinowski, S. P., Shaw, R. A., and Stratmann, F.: Can we understand clouds without turbulence?, Science, 327, 970–971, doi:10.1126/science.1185138, 2010.

Boucher, O.: The sulfate-CCN-cloud albedo effect. A sensitivity study with two general circulation models, Tellus B, 47, 281–300, 1995.

Che, H., Xia, X., Zhu, J., Li, Z., Dubovik, O., Holben, B., Goloub, P., Chen, H., Estelles, V., Cuevas-Agulló, E., Blarel, L., Wang, H., Zhao, H., Zhang, X., Wang, Y., Sun, J., Tao, R.,

ACPD
15, 15755–15790, 2015

Zhang, X., and Shi, G.: Column aerosol optical properties and aerosol radiative forcing during a serious haze-fog month over North China Plain in 2013 based on ground-based sunphotometer measurements, Atmos. Chem. Phys., 14, 2125–2138, doi:10.5194/acp-14-2125-2014, 2014.

Chen, D. H., Xue, J. S., Yang, X. S., Zhang, H. L., Shen, X. S., Hu, J. L., Wang, Y., Ji, L. R., and Chen, J. B.: New generation of multiscale NWP system (GRAPES): general scientific design, Chinese Sci. Bull., 53, 3433–3445, 2008.

Cheng, Y., Lohmann, U., and Zhang, J.: Contribution of changes in sea surface temperature and aerosol loading to the decreasing precipitation trend in southern China, J. Climate, 18, 1381–1390, 2005.

Clark, T. L.: A study in cloud phase parameterization using teh gamma distribution, J. Atmos. Sci., 31, 142–155, 1974.

Cohard, J.-M. and Pinty, J.-P.: A comprehensive two-moment warm microphysical bulk scheme. I: Description and tests, Q. J. Roy. Meteor. Soc., 126, 1815–1842, 2000.

Fan, J., Leung, L. R., Li, Z., Morrison, H., Chen, H., Zhou, Y., and Wang, Q.: Aerosol impacts on clouds and precipitation in eastern China: results from bin and bulk microphysics, J. Geophys. Res., 117, D00K36, doi:10.1029/2011JD016537, 2012.

Fritsch, J. M. and Chappell, C. F.: Numerical prediction of convectively driven mesoscale pressure systems. Part 1: Convective parameterization, J. Atmos. Sci., 37, 1722–1733, 1980.

Fuzzi, S., Andreae, M. O., Huebert, B. J., Kulmala, M., Bond, T. C., Boy, M., Doherty, S. J., Guenther, A., Kanakidou, M., Kawamura, K., Kerminen, V.-M., Lohmann, U., Russell, L. M., and Pöschl, U.: Critical assessment of the current state of scientific knowledge, terminology, and research needs concerning the role of organic aerosols in the atmosphere, climate, and global change, Atmos. Chem. Phys., 6, 2017–2038, doi:10.5194/acp-6-2017-2006, 2006.

Geoffroy, O., Brenguier, J.-L., and Burnet, F.: Parametric representation of the cloud droplet spectra for LES warm bulk microphysical schemes, Atmos. Chem. Phys., 10, 4835–4848, doi:10.5194/acp-10-4835-2010, 2010.

Ghan, S. J., Chuang, C. C., and Penner, J. E.: A parameterization of cloud droplet nulceation. Part I: Single aerosol type, Atmos. Res., 30, 197–221, 1993.

Ghan, S. J., Chuang, C. C., Easter, R. C., and Penner, J. E.: A parameterization of cloud droplet nucleation. Part II: Multiple aerosol types, Atmos. Res., 36, 39–45, 1995.

ACPD
15, 15755–15790, 2015

Gilleland, E., Ahijevych, D., Brown, B. G., Casati, B., and Ebert, E.: Intercomparison of statial forecast verification methods, Weather Forecast., 24, 1416–1430, doi:10.1175/2009WAF2222269.1, 2009.

Gong, S. L., Barrie, L. A., Blanchet, J.-P., Salzen, K. v., Lohmann, U., Lesins, G., Spacek, L., Zhang, L. M., Girard, E., Lin, H., Leaitch, R., Leighton, H., Chylek, P., and Huang, P.: Canadian aerosol module: a size-segregated simulation of atmospheric aerosol processes for climate and air quality models 1. Module development, J. Geophys. Res., 108, 4007, doi:10.1029/2001JD002002, 2003.

Gultepe, I. and Isaac, G. A.: The relationship between cloud droplet and aerosol number concentrations for climate models, Int. J. Climatol., 16, 941–946, 1996.

Guo, X., Fu, D., Guo, X., and Zhang, C.: A case study of aerosol impacts on summer convective clouds and precipitation over northern China, Atmos. Res., 142, 142–157, doi:10.1016/j.atmosres.2013.10.006, 2014.

Hayder, A.-R. and Ghan, S. J.: A parameterization of aerosol activation. 2. Multi aerosol types, J. Geophys. Res., 105, 6837–6844, 2000.

Horton, D. E., Skinner, C. B., Singh, D., and Diffenbaugh, N. S.: Occurrence and persistence of future atmospheric stagnation events, Nature Clim. Change, 4, 698–703, doi:10.1038/nclimate2272, 2014.

Houze, R. A.: Stratiform precipitation in regions of convection: a meteorological paradox?, B. Am. Meteorol. Soc., 78, 2179–2196, 1997.

Jacobson, M. C., Hansson, H.-C., Noone, K. J., and Charlson, R. J.: Organic atmospheric aerosols: review and state of the science, Rev. Geophys., 38, 267–294, 2000.

Jacobson, M. Z., Turco, R. P., Jensen, E. J., and Toon, O. B.: Modeling coagulation among particles of different composition and size, Atmos. Environ., 28, 1327–1338, 1994.

Kain, J. S.: The Kain–Fritsch convective parameterization: an update, J. Appl. Meteorol., 43, 170–181, 2003.

Kain, J. S. and Fritsch, J. M.: A one-dimensional entertaining/detraining plume model and its application in convective parameterization, J. Atmos. Sci., 47, 2784–2802, 1990.

Kalnay, E., Kanamitsu, M., Kistler, R., Collins, W., Deaven, D., Gandin, L., Iredell, M., Saha, S., White, G., Woollen, J., Zhu, Y., Chelliah, M., Ebisuzaki, W., Higgins, W., Janowiak, J., Mo, K. C., Ropelewski, C., Wang, J., Leetmaa, A., Reynolds, R., Jenne, R., and Joseph, D.: The NCEP/NCAR 40-year reanalysis project, B. Am. Meteorol. Soc., 77, 437–471, 1996.

ACPD
15, 15755–15790, 2015

Khain, A. and Sednew, I.: Simulation of precipitation formation in the eastern Mediterranean coastal zone using a spectral microphysics cloud ensemble model, Atmos. Res., 43, 77–110, 1996.
Khain, A., Ovtchinnikov, M., Pinsky, M., Pokrovsky, A., and Krugliak, H.: Notes on the state-of-art numerical modeling of cloud microphysics, Atmos. Res., 55, 159–224, 2000.
Khain, A., Pokrovsky, A., and Pinsky, M.: Simulation of effects of atmospheric aerosols on deep turbulent convective clouds using a spectral microphysics mixed-phase cumulus cloud model. Part 1: Model description and possible applications, J. Aerosol Sci., 61, 2963–2981, 2004.
Khain, A. P.: Notes on state-of-art investigations of aerosol effects on precipitation: a critical review, Environ. Res. Lett., 4, 015004, doi:10.1088/1748-9326/4/1/015004, 2009.
Khairoutdinov, M. and Kogan, Y.: A new cloud physics parameterization in a large-eddy simulation model of marine stratocumulus, Mon. Weather Rev., 128, 229–243, 2000.
Kogan, Y. L.: The simulation of a convective cloud in a 3-D model with explict microphysics. Part 1: Model description and sensitivity experiments, J. Atmos. Sci., 48, 1160–1189, 1991.
Levin, Z. and Cotton, W. R.: Aerosol Pollution Impact on Precipitation, A Scientific Review, Springer, the Netherlands, 2009.
Lim, K.-S. S. and Hong, S.-Y.: Development of an effective double-moment cloud microphysics scheme with prognostic Cloud Condensation Nuclei (CCN) for weather and climate models, Mon. Weather Rev., 138, 1587–1612, doi:10.1175/2009MWR2968.1, 2010.
Lohmann, U. and Feichter, J.: Global indirect aerosol effects: a review, Atmos. Chem. Phys., 5, 715–737, doi:10.5194/acp-5-715-2005, 2005.
Long, A. B.: Solutions to the droplet collection equation for polynomail kernels, J. Atmos. Sci., 31, 1041–1057, 1974.
Ma, J., Chen, Y., Wang, W., Yan, P., Liu, H., Yang, S., Hu, Z., and Lelieveld, J.: Strong air pollution causes widespread haze-cloud over China, J. Geophys. Res., 115, D18204, doi:10.1029/2009JD013065, 2010.
Mitternaier, M., Roberts, N., and Thompson, S. A.: A long-term assessment of precipitation forecast skill using the fractions skill score, Meterol. Appl., 20, 176–186, doi:10.1002/met.1296, 2013.
Molinari, J. and Dudek, M.: Parameterization of convective prediction in mesoscale numberical models: a critical review, Mon. Weather Rev., 120, 326–344, 1992.

ACPD
15, 15755–15790, 2015

Morrison, H., Curry, J. A., and Khvorostyanov, V. I.: A new double-moment microphysics parameterization for application in cloud and climate models. Part I: Description, J. Atmos. Sci., 62, 1665–1677, 2005.
Ogura, Y. and Cho, H.-R.: Diagnostic determination of cumulus cloud populations from observed large-scale variables, J. Atmos. Sci., 30, 1276–1286, 1973.
Ramanathan, V., Crutzen, P. J., Kiehl, J. T., and Rosenfeld, D.: Atmosphere – aerosols, climate, and the hydrological cycle, Science, 294, 2119–2124, 2001.
Seifert, A. and Beheng, K. D.: A double-moment parameterization for simulating autoconversion, accretion and self-collection, Atmos. Res., 59, 265–281, 2001.
Seinfeld, J. H. and Pandis, S. N.: Atmospheric Chemistry and Physics: from Air Pollution to Climate Change, John Wiley & Sons, Inc., New York, 1997.
Stevens, B. and Feingold, G.: Untangling aerosol effects on clouds and precipitation in a buffered system, Nature, 461, 607–613, doi:10.1038/nature08281, 2009.
Stockwell, W. R., Middleton, P., Change, J. S., and Tang, X.: The second generation regional acid deposition model chemical mechanizm for regional ai quality modeling, J. Geophys. Res., 95, 16343–16376, 1990.
Stockwell, W. R., Kirchner, F., Kuhn, M., and Seefeld, S.: A new mechanism for regional atmospheric chemistry modeling, J. Geophys. Res., 102, 25847–25879, 1997.
Tao, W.-K., Chen, J.-P., Li, Z., Wang, C., and Zhang, C.: Impact of aerosols on convective clouds and precipitation, Rev. Geophys., 50, RG2001, doi:10.1029/2011RG000369, 2012.
Twomey, S.: The nuclei of natural cloud formation, II, The supersaturation in natural clouds and the variation of cloud droplet concentration, Geofisica Pura Applicata, 43, 243–249, 1959.
Twomey, S. J.: The influence of pollution on the shortwave albedo of clouds, J. Atmos. Sci., 34, 1149–1152, 1977.
Walko, R. L., Cotton, W. R., Meyers, M. P., and Harrington, J. Y.: New RAMS cloud microphysics parameterization Part 1: The single-momnet scheme, Atmos. Res., 38, 29–62, 1995.
Wang, H., Zhang, X.Gong, S., Chen, Y., Shi, G., and Li, W.: Radiative feedback of dust aerosols on the East Asian dust storms, J. Geophys. Res., 115, D23214, doi:10.1029/2009JD013430, 2010.
Wang, H., Shi, G. Y., Zhang, X. Y., Gong, S. L., Tan, S. C., Chen, B., Che, H. Z., and Li, T.: Mesoscale modelling study of the interactions between aerosols and PBL meteorology during a haze episode in China Jing–Jin–Ji and its near surrounding region – Part 2: Aerosols'

ACPD
15, 15755–15790, 2015

radiative feedback effects, Atmos. Chem. Phys., 15, 3277–3287, doi:10.5194/acp-15-3277-2015, 2015.
Wang, J. Z., Gong, S. L., Zhang, X. Y., Yang, Y. Q., Hou, Q., Zhou, C. H., and Q. Wang, Y.: A Parameterized Method for Air-Quality Diagnosis and Its Applications, Adv. Meteorol., 2012, 238589, doi:10.1155/2012/238589, 2012.
Wang, Y., Yao, L., Wang, L., Liu, Z., Ji, D., Tang, G., ZHang, J., Sun, Y., Hu, B., and Xin, J.: Mechanism for the formation of the January 2013 heavy haze pollution episode over central and eastern China, Sci. China Ser. D, 57, 14–25, doi:10.1007/s11430-013-4773-4, 2014.
Wang, Y. Q., Zhang, X. Y., Gong, S. L., Zhou, C. H., Hu, X. Q., Liu, H. L., Niu, T., and Yang, Y. Q.: Surface observation of sand and dust storm in East Asia and its application in CUACE/Dust, Atmos. Chem. Phys., 8, 545–553, doi:10.5194/acp-8-545-2008, 2008.
Xu, G. Q., Chen, D. H., Xue, J. S., Sun, J., Shen, X. S., Shen, Y. F., Huang, L. P., Wu, X. J., Zhang, H. L., and Wang, S. Y.: The program structure designing and optimizing tests of GRAPES physics, Chinese Sci. Bull., 53, 3470–3476, 2008.
Yang, S., Ma, J., Hu, Z., Yan, P., Chen, Y., and Wang, W.: Influence of multi-chemical-component aerosols on the microphysics of warm clouds in north China, Sci. China Ser. D, 54, 451–461, doi:10.1007/s11430-010-4075-z, 2011.
Yin, Y., Wurzler, S., Levin, Z., and Reisin, T. G.: Interactions of mineral dust particles and clouds: effects on precipitation and cloud optical properties, J. Geophys. Res., 107, 4724, doi:10.1029/2001JD001544, 2002.
Zhang, D., Guo, X., Gong, D., and Yao, Z.: The observational results of the clouds microphysical structure based on the data obtained by 23 sorties between 1989 and 2008 in Shandong Province, Acta Meteorol. Sin., 69, 195–207, 2011.
Zhang, R., Li, G., Fan, J., Wu, D. L., and Molina, M. J.: Intensification of Pacific storm track linked to Asian pollution, P. Natl. Acad. Sci. USA, 104, 5295–5299, doi:10.1073/pnas.0700618104, 2007.
Zhang, R. H. and Shen, X. S.: On the development of the GRAPESA new generation of the national operational NWP system in China, Chinese Sci. Bull., 53, 3429–3232, 2008.
Zhang, R. H., Li, Q., and Zhang, R. N.: Meteorological conditions for the persistent severe fog and haze event over eastern China in January 2013, Sci. China Ser. D, 57, 26–35, doi:10.1007/s11430-013-4774-3, 2013.

ACPD
15, 15755–15790, 2015

Zhang, X. Y., Wang, Y. Q., Zhang, X. C., Guo, W., and Gong, S. L.: Carbonacious aerosol composition over various regions of China during 2006, J. Geophys. Res., 113, D14111, doi:10.1029/2007JD009525, 2008.

Zhang, X. Y., Wang, Y. Q., Niu, T., Zhang, X. C., Gong, S. L., Zhang, Y. M., and Sun, J. Y.: Atmospheric aerosol compositions in China: spatial/temporal variability, chemical signature, regional haze distribution and comparisons with global aerosols, Atmos. Chem. Phys., 12, 779–799, doi:10.5194/acp-12-779-2012, 2012.

Zhang, X. Y., Sun, J. Y., Wang, Y. Q., Li, W. J., Zhang, Q., Wang, W. G., Quan, J., N., Cao, G. L., Wang, J. Z., Yang, Y. Q., and Zhang, Y. M.: Factors contributing to haze and fog in China, Chinese Sci. Bull. (Chin. ver.), 58, 1178–1187, doi:10.1360/972013-150, 2013 (in Chinese).

Zhang, Y., Seigneur, C., Senfeld, H. H., Jacbson, M. Z., and Binkowski, F. S.: Simulation of aerosl dynamics: a comparative review of algorithms used in air quality models, Aerosol Sci. Tech., 31, 487–514, 1999.

Zhang, Y., Yin, Y., Shi, L., Duan, Y., and Wu, Z.: Analysis of cloud microphysics structure over Hebei region during autumn of 2007, Plateau Meteorology, 31, 530–537, 2012 (in Chinese).

Zhao, C., Tie, X., and Lin, Y.: A possible positive feedback of reduction of precipitation and increase in aerosols over eastern central China, J. Geophys. Res., 33, L11814, doi:10.1029/2006GL025959, 2006.

Zhou, C. H., Gong, S. L., Zhang, X. Y., Wang, Y. Q., Niu, T., Liu, H. L., Zhao, T. L., Yang, Y. Q., and Hou, Q.: Development and evaluation of an operational SDS forecasting system for East Asia: CUACE/Dust, Atmos. Chem. Phys., 8, 787–798, doi:10.5194/acp-8-787-2008, 2008.

Zhou, C.-H., Gong, S., Zhang, X.-Y., Liu, H. L., Xue, M., Cao, G. L., An, X. Q., Che, H. Z., Zhang, Y. M., and Niu, T.: Towards the improvements of simulating the chemical and optical properties of Chinese aerosols using an online coupled model CUACE/Aero, Tellus B, 64, 18965, doi:10.3402/tellusb.v64i0.18965, 2012.

ACPD
15, 15755–15790, 2015

Table 1. TS scoring comparisons for eight precipitation events for T1, T2 and T3.

CASES	time period (dd.hh)	T3	T2	T1	(T3 – T1)/ T1 · 100 %	(T2 – T1)/ T1 · 100 %
1	2.12–7.06	0.518	0.334	0.326	58.9	2.5
2	7.18–9.12	0.314	0.281	0.333	−5.7	−15.6
3	10.06–13.06	0.482	0.252	0.327	47.4	−22.9
4	14.12–17.18	0.417	0.185	0.224	86.2	−17.4
5	23.00–24.18	0.403	0.151	0.213	89.2	−29.1
6	25.18–27.12	0.436	0.144	0.149	192.6	−3.4
7	19.06–22.12	0.532	0.349	0.389	36.8	−10.3
8	29.06–31.00	0.469	0.27	0.338	38.8	−20.1

ACPD
15, 15755–15790, 2015

Table 2. Biases for the five regions of R1–R5 and three tests T1–T3.

	R1	R2	R3	R4	R5
T1	0.73	0.62	0.55	0.60	0.60
T2	0.75	0.63	0.95	0.80	0.54
T3	1.13	1.11	0.92	0.90	1.19

ACPD
15, 15755–15790, 2015

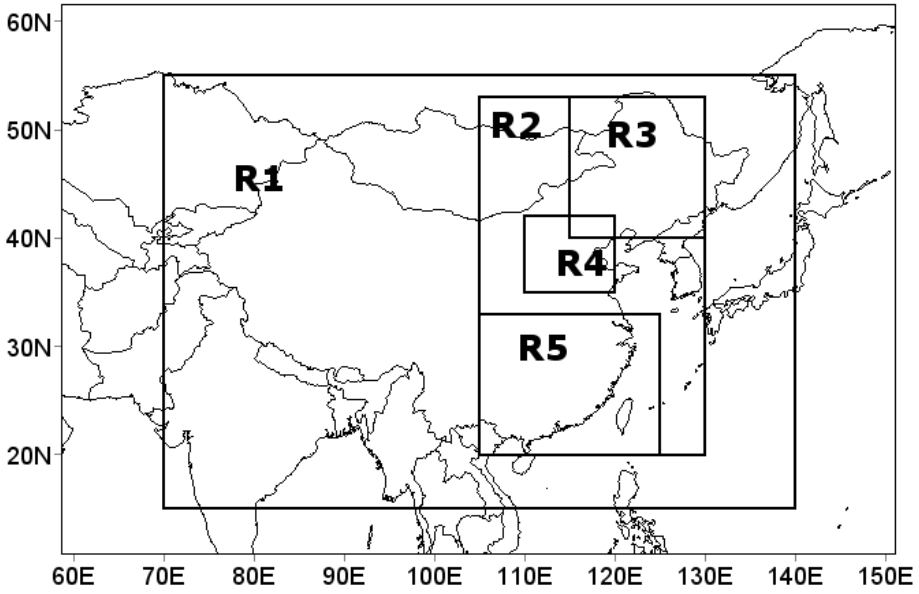

Figure 1. Model domain and five targeting areas. R1 is for the whole China, R2 is for east China, R3 is for northeast China, R4 is for North China Plain and R5 is for south China.

ACPD
15, 15755–15790, 2015

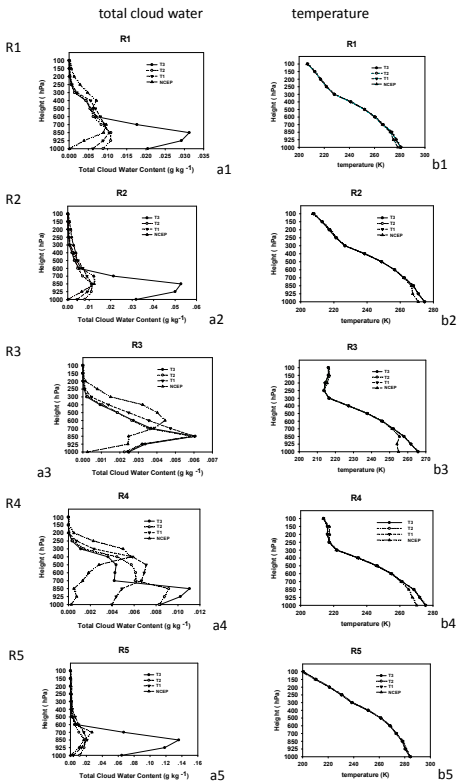

Figure 2. Vertical profiles of regional mean total cloud water content **(a1–a5)** and temperature **(b1–b5)** from 1000 to 100 hPa for R1, R2, R3, R4 and R5. T1 is for WSM6, the control test, T2 is for WDM6 with K2000 activation scheme, T3 is for WDM6 with aerosol activated from CUACE. NCEP is for NCEP reanalysis.

ACPD
15, 15755–15790, 2015

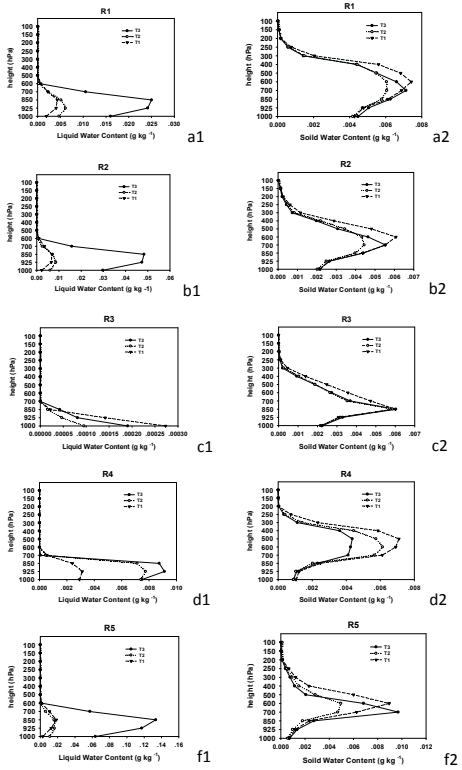

Figure 3. Vertical profiles of regional mean liquid water **(a1–f1)** and solid water **(a2–f2)** for R1, R2, R3, R4 and R5 from 1000 to 100 hPa. T1 is for WSM6, the control test, T2 is for WDM6 with K2000 activation scheme, T3 is for WDM6 with aerosol activated from CUACE. NCEP is for NCEP reanalysis.

ACPD
15, 15755–15790, 2015

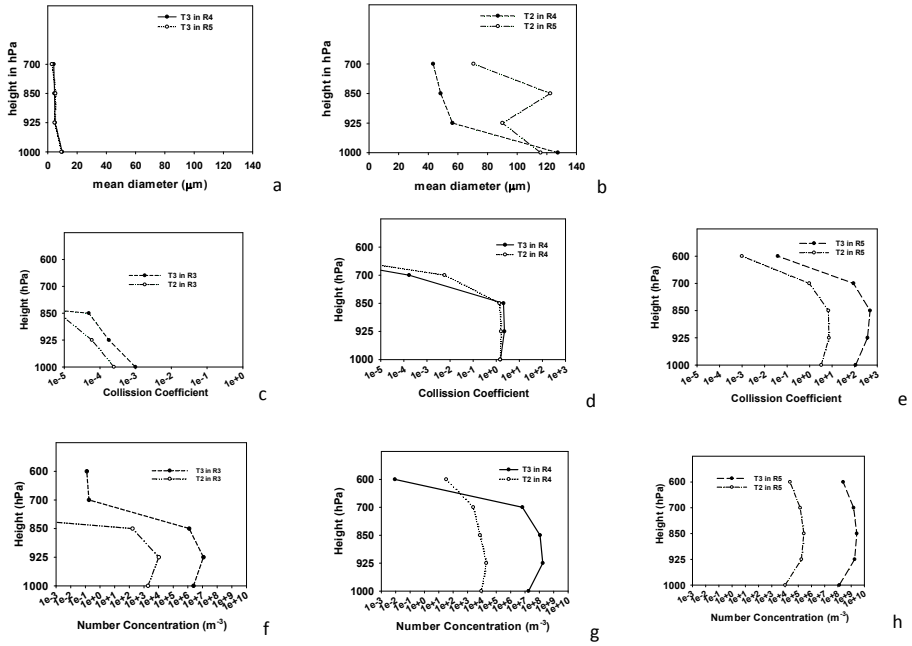

Figure 4. (a) is the vertical profile of mean diameter of cloud droplets for T3 in R4 and R5, **(b)** is same to **(a)** but for T2. **(c)** is collision coefficient for T2 and T3 in R3, **(d)** and **(e)** are same to **(c)** but for R4 and R5. **(f)** is cloud droplet number concentration for T2 and T3 in R3, **(g)** and **(h)** are the same to **(f)** but for R4 and R5.

ACPD
15, 15755–15790, 2015

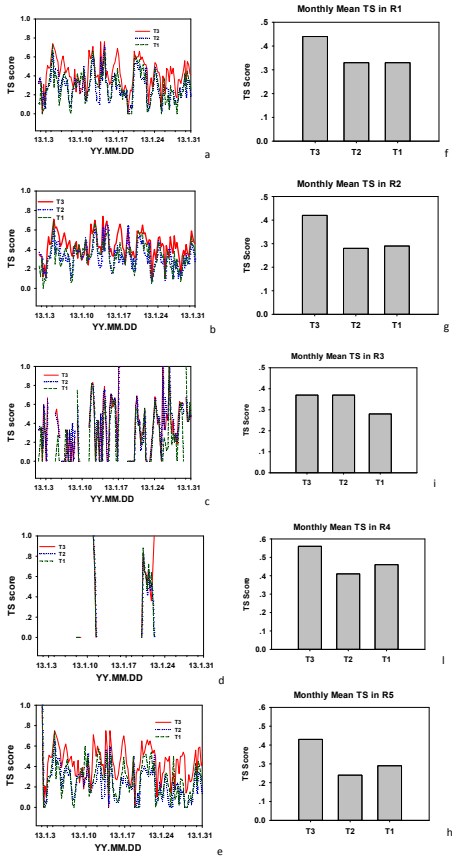

Figure 5. Time series of 6 h precipitation TS scoring **(a–e)** and monthly mean TS score **(f–h)** for R1, R2, R3, R4, R5. T1 is for WSM6, the control test, T2 is for WDM6 with K2000 activation scheme, T3 is for WDM6 with aerosol activated from CUACE.

ACPD
15, 15755–15790, 2015

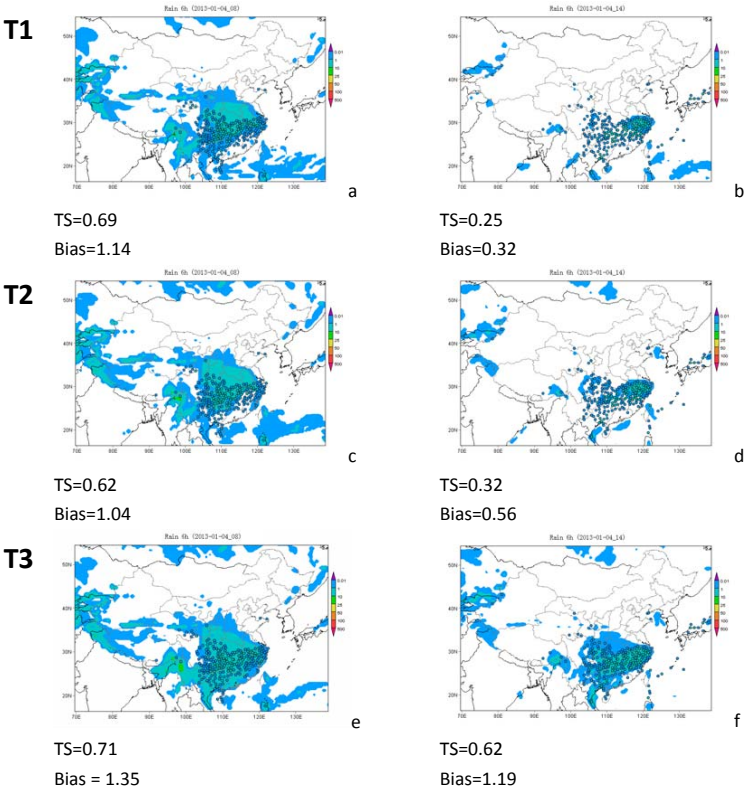

Figure 6. (a) is the distribution of 6 h accumulated precipitation(shaded) compared with observation(dotted) with the TS scoring and bias at 08:00 LT 4 January 2013 by T1. **(b)** is the same to **(a)** but for 14:00 LT, **(c)** is the same to **(a)** but for T2, **(d)** is same to **(c)** but for 14:00 LT. **(f)** is the same to **(a)** but for T3, **(f)** is the same to **(e)** but for 14:00 LT.

ACPD
15, 15755–15790, 2015

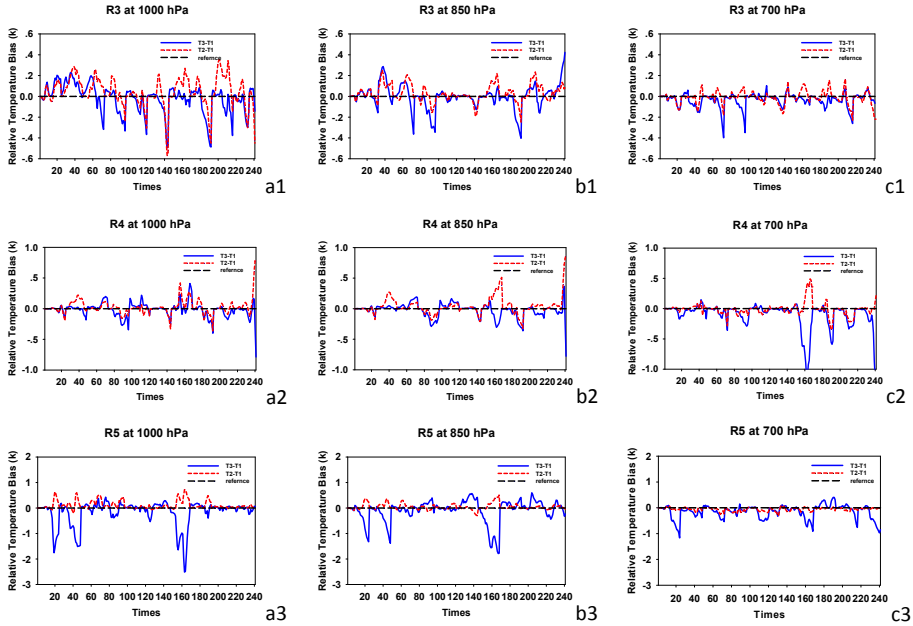

Figure 7. Temperature bias differences between T3 and T1, T2 and T1 at three heights of 1000, 850 and 700 hPa for the three regions of R3, R4 and R5.

ACPD
15, 15755–15790, 2015

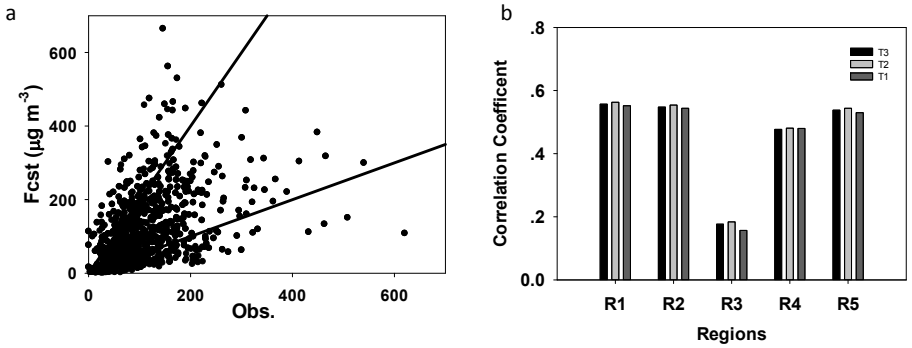

Figure 8. (a) Correlation coefficients of $PM_{2.5}$ between simulation and measurements for T1, T2 and T3 in five regions of R1, R2, R3, R4 and R5. **(b)** Scatter plot of daily average $PM_{2.5}$ between the model and the observations for T3 in R1.

ACPD
15, 15755–15790, 2015